MoS_2/VO_2 vdW heterojunction devices: tunable rectifiers, photodiodes and field effect transistors

N. Oliva[1], E. A. Casu[1], C. Yan[2], A. Krammer[3], A. Magrez[4], A. Schueler[3], O. J. F. Martin[2] and A. M. Ionescu[1]
[1]Nanoelectronic Device Laboratory (Nanolab), [2]Nanophotonics and Metrology Laboratory (NAM), [3]Solar Energy and Building Physics Laboratory and [4]Istitut de Physique, EPFL, Lausanne, Switzerland.

***Abstract*—**In this work we report a new class of ultra-thin film devices based on n-n van der Waals (vdW) heterojunctions of MoS_2 and VO_2, which show remarkable tunable characteristics. The favorable band alignment combined with the sharp and clean vdW interface determines a tunable diode-like characteristic with a rectification ratio larger than 10^3. Moreover, the heterojunction can be turned into a Schottky rectifier with higher on-current by triggering the VO_2 insulator to metal transition (IMT), by either applying a sufficiently large voltage or increasing the temperature above 68 °C. The proposed devices are photosensitive with linear photoresponse and temperature tunable photoresponsivity values larger than 1 in the 500/650 nm wavelength range.

We finally report the first ever field-effect transistor based on gated MoS_2/VO_2 heterojunctions, which is a true low power FET exploiting a phase change material where the electrostatic doping effect of the gate on the junction results in a subthreshold slope (SS) of 130 mV/dec at room temperature, $I_{ON}/I_{OFF} > 10^3$ and $I_{OFF} < 5$ pA/μm at V_D=1.5V.

I. Introduction

Vanadium dioxide (VO_2) is a strongly correlated functional oxide exhibiting an insulator to metal transition (IMT) resulting in a high conductivity contrast between the two phases. This transition can be induced by electrical excitation, making VO_2 an ideal candidate for the realization of solid state devices. Two-terminal switches have been thoroughly characterized, exhibiting steep transition characteristic and fast switching time [1]. Three-terminal devices based on VO_2 as semiconductor channel have been proposed and demonstrated, but they resulted in an extremely limited electrostatic control on channel conductance and IMT threshold temperature [2]. A better control has been achieved by connecting a discrete VO_2 switch in series with either the source or gate of a silicon based FET, where the steep VO_2 IMT transition is used to overcome the thermal limit of 60 mV/dec [3, 4]. However, problems related to the achieved I_{ON}/I_{OFF} ratio and the power consumption have still to be addressed.

Here, we propose for the first time a new class of devices based on the heterojunction between molybdenum disulphide (MoS_2) and VO_2. Two-terminal devices exhibit good current rectification performance and excellent optical responsivity, both tunable in temperature thanks to the strongly temperature dependent properties of VO_2. Moreover, we demonstrate the possibility of inducing the VO_2 IMT by electrical excitation at room temperature, obtaining a stable and reversible switching of the VO_2 side of the junction. Finally, we demonstrate the first field-effect devices based on the MoS_2/VO_2 heterojunction, obtaining a good electrostatic control on the junction conduction and a substantial reduction of the I_{OFF} current with respect to three terminal devices based on VO_2 channels [2].

II. Fabrication

The process flow designed for the fabrication of MoS_2/VO_2 heterojunction devices is summarized in Fig. 1a. A 75 nm thick VO_2 film was deposited by reactive sputtering on a silicon substrate with a 2 μm thick wet oxide on top. We report in Fig. 2 the XRD spectrum obtained from the as deposited film while Fig. 3 shows the resistivity curve of the film vs temperature, demonstrating a hysteretic IMT around 68 °C. Reference VO_2 switches fabricated on this film exhibit a reversible and stable electrically induced IMT, as shown in Fig. 4. We patterned the VO_2 film by electron beam lithography (EBL) and wet etching.

The MoS_2 bulk crystals were synthesized in EPFL crystal growth facility [5]. We mechanically exfoliated the MoS_2 flakes on a PDMS stamp [6], used to transfer them on the edge between pre-patterned VO_2 structures and the exposed SiO_2 layer. The results reported in the following have been obtained with MoS_2 flakes with thickness ranging from 40 to 100 nm. Two-terminal devices were completed with a further EBL step and lift-off of 100 nm thick gold contacts on the two sides of the junction. A schematic view of the structure is depicted in Fig. 1b together with an optical image (inset).

Top-gated devices required the deposition of a dielectric layer. An Al_2O_3 seed layer was deposited by sputtering and oxidizing at 180°C in ambient atmosphere a 2 nm thick Al layer, followed by the deposition of 5 nm of HfO_2 by ALD. The gate contact was obtained by EBL and lift-off of 1 nm Ta and 140 nm Au. Fig. 1c shows a schematic view and an optical image (inset) of the complete device.

III. Diode and Photodiode Characterization

The qualitative band diagram for the heterojunction of multilayer MoS_2 and VO_2 is depicted in Fig. 5. When VO_2 is in the insulating state (Fig. 5a), both the materials are intrinsically n-type semiconductors [7, 8]. The discontinuity in the conduction band (ΔE_C) is estimated to be 1 eV according to the affinity rule, while the built-in voltage is estimated to be in the 0.35/0.75 eV range. The band diagram of the junction with VO_2 in the metallic phase presents a Schottky barrier comparable to ΔE_C (Fig. 5b).

The I-V curve of a representative heterojunction at room temperature, obtained grounding the contact on MoS_2 and sweeping the voltage on the VO_2, is shown in Fig. 6. A clear rectifier behavior is observed, with a rectification ratio larger than 10^3. By applying a positive bias to VO_2, electron injection from MoS_2 conduction band is favored resulting in the exponential increase of the current. Conversely, under reverse bias electrons to be injected from VO_2 to MoS_2 face the large ΔE_C barrier (Fig. 5a). The device characteristic close to 0 V can be described using the ideal diode model, resulting in an ideality factor of 1.75 as shown in Fig. 7. A better description of the non-saturating reverse current can be obtained using the Fang-Howard model [9], specifically

developed for rectifying n-n heterojunctions and based on the introduction of a voltage dependent I_S expression (inset of Fig. 7).

Temperature impact on heterojunction conduction was investigated measuring I-V curves at increasing temperatures as shown in Fig. 8. A gradual increase of both forward and reverse current was observed below the IMT temperature. Above the transition temperature, the current increase tends to saturate. The heterojunction with metallic VO_2 is still rectifying, exhibiting same rectification ratio and larger forward current with respect to the junction with insulating VO_2. The evolution of the extracted diode ideality factor and saturation current is shown in Fig. 9. The ideality factor increases approaching the IMT temperature, while it decreases above it, similarly to what has been reported for GaN/VO_2 heterojunctions [7].

Upon exposure to light, the device characteristic is shifted resulting in a non zero open circuit voltage (V_{OC}) and short circuit current (I_{SC}) as shown in Fig. 10. Moreover, the photoresponse is linear with respect to the incident light power density as reported in Fig. 11. Transient photoresponse measurements (inset of Fig. 11) resulted in an extracted decay time of 3.5 ms.

Fig. 12 shows the spectral evolution of the device responsivity, measured at increasing temperatures. The cut-off wavelength is located between 750 and 800 nm, suggesting the light absorption takes place mostly in the MoS_2 side of the heterojunction [10]. Responsivity is clearly boosted by the increase of temperature. The enhancement of the photoresponse can be due to different mechanisms: larger built in voltage because of the increased work function of metallic VO_2; increase of the depletion region in the MoS_2 side; enhanced optical absorption due to interference effects related to the variation of VO_2 optical properties [11]. The heterojunction behaves as a photodiode with temperature tunable photoresponse, reaching responsivity values larger than 1 in the 500/650 nm range. The electrical power (P_{el}) generated by the photodiode is found to decrease at the increase of the temperature, as shown in Fig. 13. Upon heating, the short circuit current I_{SC} increases at a lower rate with respect to the open circuit voltage V_{OC} decrease (Fig. 15), causing the overall P_{el} to decrease [10].

A reversible electrically triggered IMT was demonstrated on a second device at room temperature (Fig. 15). The high actuation voltage is due to the resistance offered by the heterojunction and the sum of the series resistances in the structure. We verified that the electrically triggered IMT did not alter the heterojunction conduction by comparing in Fig. 16 the I-V curve before and after the experiment.

IV. Three Terminal Devices

Finally, we realized and characterized three terminal devices. Fig. 17 shows the I-V characteristic of a diode measured before and after the deposition of the gate stack. An applied negative gate bias determines a significant reduction of forward current and rectification ratio as reported in Fig. 18. Fig. 19 shows drain current and output conductance measured at different gate bias values. The output characteristic shows no saturation in the considered range of drain voltage. The impact of gate bias on the junction conduction can be explained in terms of the qualitative band diagram depicted in Fig. 20. For $V_G < 0$, MoS_2 bands are shifted upward in the gated region, resulting in a depletion of electrons and a reduction of the diode forward current and output conductance.

The transfer characteristic of a second device measured at a drain bias of 1.5 V is reported in Fig. 21 together with the gate leakage current and the transconductance. The heterojunction transistor shows a n-type depletion mode conduction with a I_{ON}/I_{OFF} ratio of three orders of magnitude, limited by the series and junction resistances, and an I_{OFF} as low as 4.7 pA/μm. The extracted transconductance shows a narrow peak due to the observed current saturation. Fig. 22 reports the device subthreshold slope as a function of the drain current: a minimum value of 130 mV/dec is achieved and maintained over almost two decades of the output current. The double sweep transfer characteristic in the inset shows a 300 mV hysteresis.

V. Conclusions

We have demonstrated a novel class of devices based on the n-n heterojunction between MoS_2 and VO_2. Two-terminal devices behave as current rectifiers, with rectification ratio larger than 10^3. We validated the heterojunction performance as photodiode, obtaining a linear photoresponse and an excellent temperature dependent responsivity. Two-terminal devices were used to prove the possibility of triggering a reversible IMT of the VO_2 side of the junction at room temperature, by applying a sufficiently large forward bias. Finally, we realized the first FETs with phase change semiconductor heterojunction showing excellent gate control and ultra-low I_{OFF} current.

The presented results demonstrate the possibility of exploiting VO_2 in order to finely tune and enhance the electrical and optical properties of heterojunctions with other semiconductor materials, opening interesting opportunities in particular for sensing applications. Moreover, the demonstrated gate control over the junction conduction paves the way for the realization of field effect solid state devices based on VO_2. Reducing the threshold voltage required for the IMT it would be possible to trigger the phase transition at low drain biases, relying on the effect of the gate field so to obtain a novel approach for the realization of sub-thermionic steep-slope devices.

Acknowledgment

This work was financially supported by the European Research Council (ERC) under the ERC Advanced Grants Milli-Tech (ERC-2015-AdG-695459) and Nanofactory (ERC-2015-AdG-695206), by the Swiss National Science Foundation (Grant No. 200021_162453) and by the Swiss Federal Office of Energy (Grant No. 8100072).

References

[1] J. Leroy *et al.*, "High-speed metal-insulator transition in vanadium dioxide films induced by an electrical pulsed voltage over nano-gap electrodes," *Appl. Phys. Lett.*, vol. 100, no. 21, p. 213507, 2012.

[2] D. Ruzmetov *et al.*, "Three-terminal field effect devices utilizing thin film vanadium oxide as the channel layer," *J. Appl. Phys.*, vol. 107, no. 11, p. 114516, 2010.

[3] N. Shukla *et al.*, "A steep-slope transistor based on abrupt electronic phase transition," *Nat. Commun.*, vol. 6, p. 7812, 2015.

[4] E.A. Casu *et al.*, "Hybrid Phase-Change – Tunnel FET (PC-TFET) Switch with Subthreshold Swing < 10mV/decade and sub-0.1 body factor: digital and analog benchmarking," *IEDM, 2016 IEEE Int.*, 2016.

[5] A. Pisoni *et al.*, "The role of transport agents in MoS2 single crystals," *J. Phys. Chem. C*, vol. 119, no. 8, pp. 3918–3922, 2015.

[6] A. Castellanos-Gomez *et al.*, "Deterministic transfer of two-dimensional materials by all-dry viscoelastic stamping," *2D Mater.*, vol. 1, no. 1, 2014.

[7] Y. Zhou *et al.*, "GaN/VO2 heteroepitaxial p-n junctions: Band offset and minority carrier dynamics," *J. Appl. Phys.*, vol. 113, no. 21, 2013.

[8] S. Das *et al.*, "High performance multilayer MoS2 transistors with scandium contacts," *Nano Lett.*, vol. 13, no. 1, pp. 100–105, 2013.

[9] F. F. Fang and W. E. Howard, "Effect of crystal orientation on Ge-GaAs heterojunctions," *J. Appl. Phys.*, vol. 35, no. 3, pp. 612–617, 1964.

[10] Svatek, S. A. *et al.* Gate Tunable Photovoltaic Effect in MoS_2 vertical P-N Homostructures. *J. Mater. Chem. C* **5,** 854–861 (2017).

[11] J. Hou, X. *et al.*, "Modulating Photoluminescence of Monolayer Molybdenum Disulfide by Metal-Insulator Phase Transition in Active Substrates," *Small*, no. 29, pp. 3976–3984, 2016.

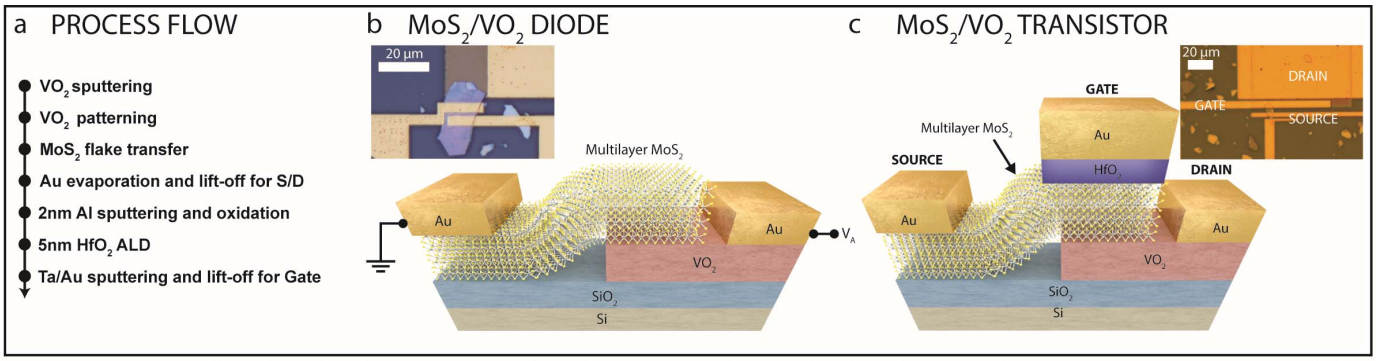

Fig. 1. (a) Main steps followed for the fabrication of MoS_2/VO_2 heterojunction devices. (b) Three dimensional schematic view of a two terminal device and optical image (inset). Three terminal devices have been obtained by depositing a Al_2O_3/HfO_2 dielectric stack and a top Ta/Au electrode, as shown in the schematic structure and optical image in (c).

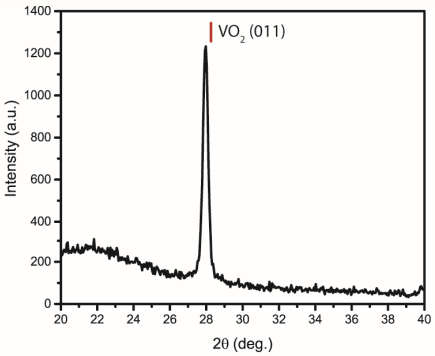

Fig. 2. XRD spectrum of the sputtered 75 nm thick VO_2 film. A clear peak is present at 28°, corresponding to VO_2 (011) plane.

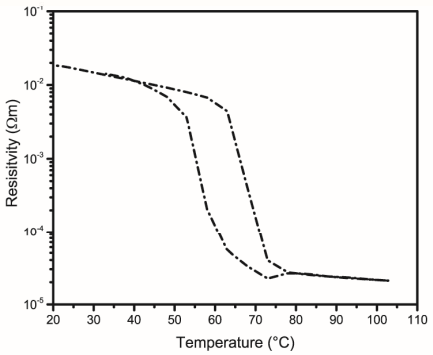

Fig. 3. Resistivity curve of the as deposited VO_2 film, showing an IMT around 68 °C and a resistivity reconfigurability of three orders of magnitude.

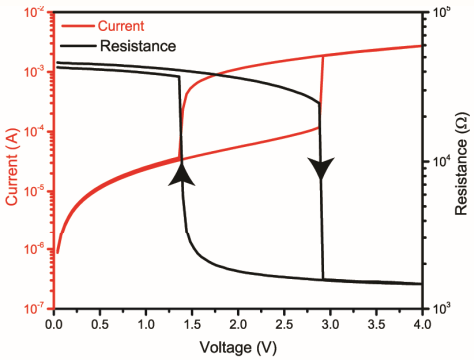

Fig. 4. Current (red) and resistance (black) characteristics of a VO_2 switch co-fabricated on the same film used for the heterojunctions.

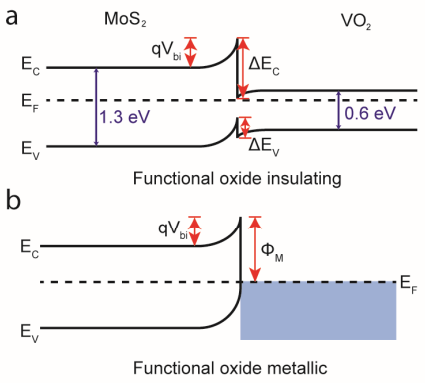

Fig. 5. Heterojunction qualitative band diagram with VO_2 in (a) the insulating phase and (b) the metallic phase.

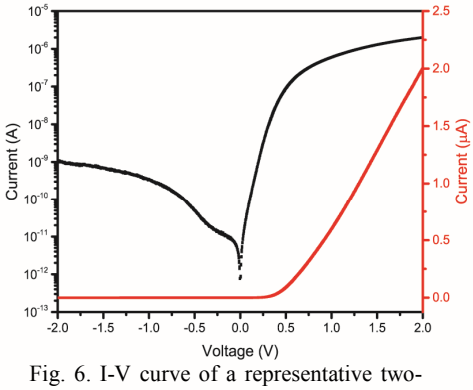

Fig. 6. I-V curve of a representative two-terminal heterojunction device in linear (red) and logarithmic (black) scale.

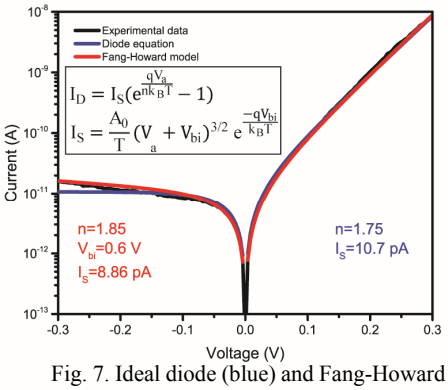

Fig. 7. Ideal diode (blue) and Fang-Howard model (red) compared to the experimental characteristic (black). The Fang-Howard model is able to describe the non-saturating reverse current by modifying I_S expression, as reported in the inset.

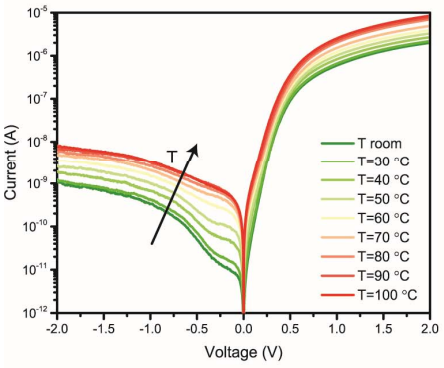

Fig. 8. Measured electrical characteristic of the heterojunction at increasing temperature.

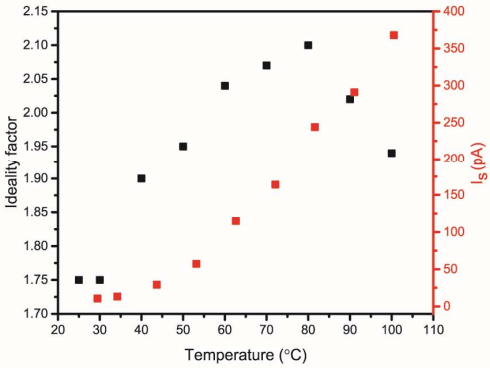

Fig. 9. Extracted diode ideality factor and saturation current as a function of temperature.

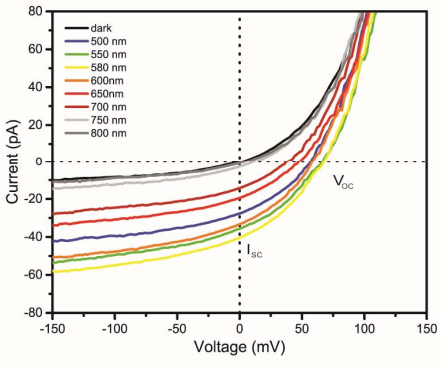

Fig. 10. I-V characteristic of the heterojunction in dark conditions and under illumination with different wavelengths at power density 330 nW/mm^2.

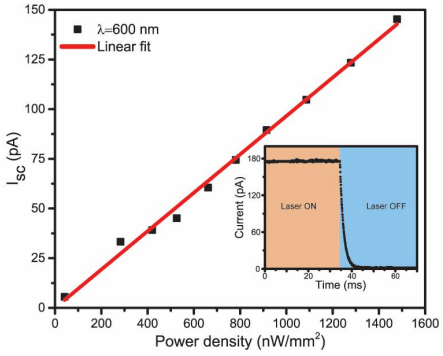

Fig. 11. Measured short circuit current under illumination at λ = 600 nm with increasing power density. Inset: transient response of the heterojunction showing a 3.5 ms decay time.

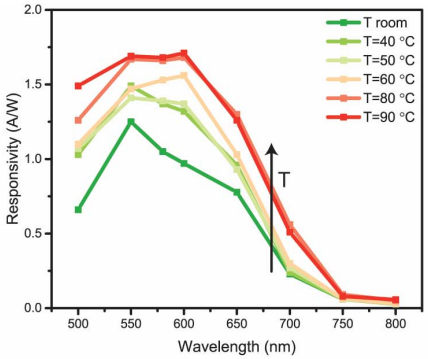

Fig. 12. Extracted photoresponsivity as a function of the illumination wavelength measured at different temperatures.

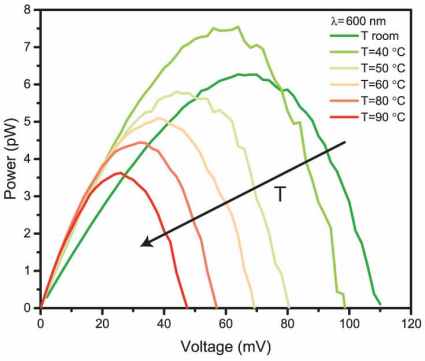

Fig. 13. Electrical power generated by the heterojunction under 600 nm light at 1.48 μm/mm^2 power density.

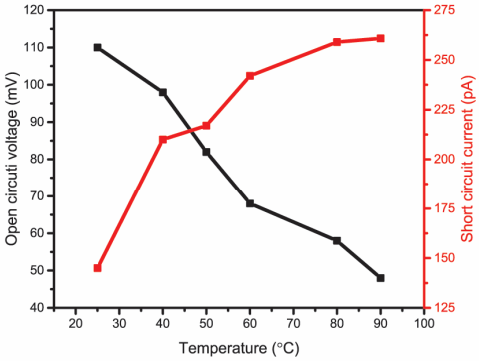

Fig. 14. Open circuit voltage and short circuit current as function of temperature under illumination at 600 nm with 1.48 μm/mm^2 power density.

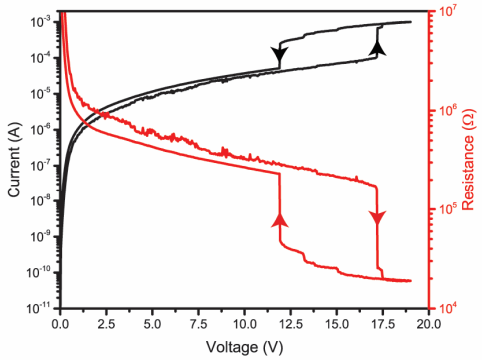

Fig. 15. Electrical characteristic at room temperature of a two terminal heterojunction device under bias large enough to trigger the VO_2 IMT.

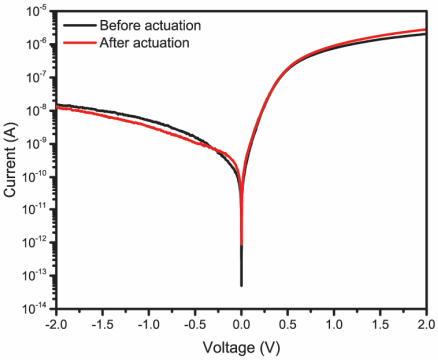

Fig. 16. I-V curve of the same device before (black) and after (red) having electrically induced VO_2 IMT.

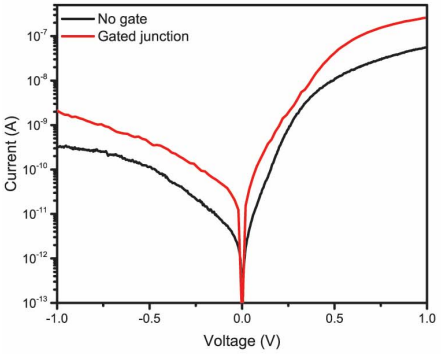

Fig. 17. Double sweep I-V curve of a two diode before and after the deposition of the gate dielectric and top metal contact.

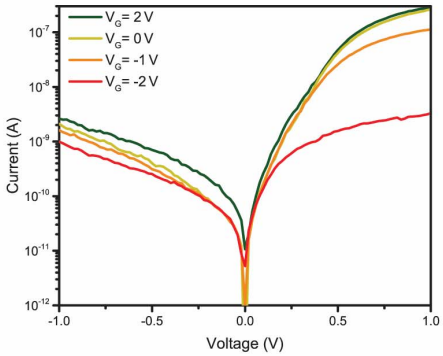

Fig. 18. Diode I-V characteristic measured at different gate bias values. A negative gate voltage determines a decrease of forward current and diode rectification ratio.

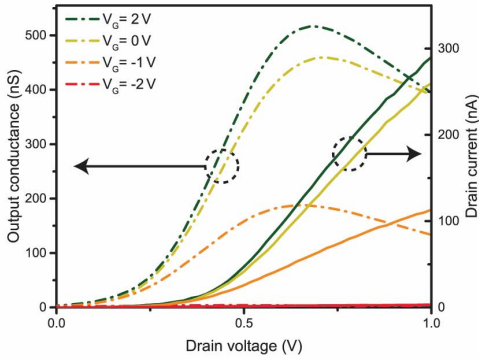

Fig. 19. Output conductance as a function of drain voltage for different values of the gate bias.

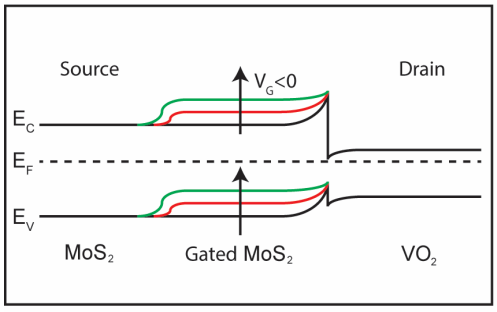

Fig. 20. Qualitative band diagram of a gated heterojunction device. A negative gate bias determines an upward shift of MoS_2 bands in the gated region and a depletion of electrons.

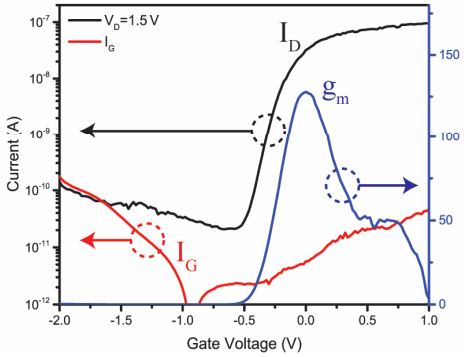

Fig. 21. Transfer characteristic (black), transconductance (blue) and gate leakage (red) of a heterojunction transistor measured at a 1.5 V drain bias. The device shows an I_{ON}/I_{OFF} ratio larger than 3 orders of magnitude.

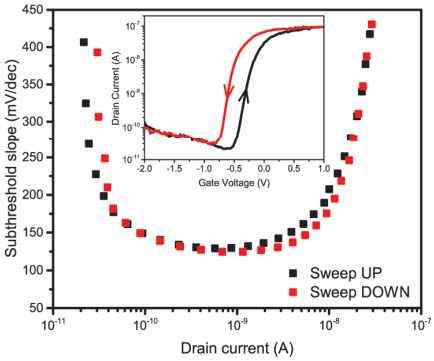

Fig. 22. Subthreshold slope of the heterojunction transistor as a function of the drain current obtained from a double sweep measurement. A SS value of 130 mV/dec is maintained over almost two decades of output current. Inset: double sweep transfer characteristic showing a 300 mV hysteresis.